

PETROGRAPHY AND GEOCHEMISTRY OF DOLERITE DYKES FROM CRETACEOUS BAMWA HALF GRABEN (NORTH CAMEROON, CENTRAL AFRICA)

ABSTRACT

Petrography and geochemistry of dolerite dykes from cretaceous Bamwa half grabben of North Cameroon in Central Africa have been done. Field work study have shown that dykes swarms of Bamwa basin exceptionally occurred as well exposed dykes vertically overhanging the local granitoids of the basement along trending direction of N155E. Dykes are 1 to 26 m wide and extend on 400 to 500 m. Microscopic observations have revealed various textures, from ophitic, sub-ophitic, classical dolerite to microlitic porphyritic. All dolerites are petrographically composed of plagioclase, oxides, clinopyroxene, rare apatite, chlorite and amphibole crystals, marked by alteration signs. ICP-AES and ICP-MS geochemical analyses of Bamwa dolerites have distinguished the dolerites lavas of basaltic trachyandesite, andesite, dacite and rhyolite composition. Bamwa dolerites are giant dykes which exhibit the geochemical characters of continental tholeiites of low TiO_2 composition ($\text{TiO}_2 < 2$ wt. %). Petrographic and geochemical studies of the dolerite dykes of Bamwa basin have shown that studied dolerites have experienced a complex petrogenetic history through assimilation and fractional crystallization, fluid infiltration and varying degrees of crustal contamination processes, after a relatively high partial melting rate of enriched subcontinental lithospheric mantle source. Studied dolerites stand as fingerprints of post Pan African magmatic events of arc-back arc setting after subduction.

Key words: *dykes swarms, continental tholeiites, crustal contamination, lithospheric mantle, arc-back arc setting, Bamwa basin, north Cameroon, central Africa.*

1. INTRODUCTION

Bamwa basin in central north Cameroon (Fig.1A) is among the E-W small basins of half grabens shape of Neocomian-early Aptian age of 130-118 Ma (Wilson & Guiraud, 1998). Those basins are distinguished by their oldest ages from large Albo-Aptian basins in the adjacent Benue Trough, Eastern Niger and southwestern Chad (Guiraud & Maurin, 1992). They have been formed from Neocomian to Early Aptian roughly E-W and NW trending troughs (Upper Benue, N Cameroon, S Chad, Sudan etc.) and have been Initiated in response to a submeridian extensional regime in Central Africa while in Western Africa the N-S trending transsaharian fault zone acted as a sinistral wrench (Guiraud & Maurin, 1992). The filling products are composed of various sedimentary rocks associated to poorly dated magmatism composed of extrusive alkaline basalts, dolerite and basaltic dykes and sills (Guiraud & Maurin, 1992). The similar magmatic even have been reported in the Upper Benue Trough, the Ghana margin and in northeastern Brazil where they are known to be occurred under the similar tectonic environments, ranging in age from 130 to 120 Ma (Wilson & Guiraud 1998, Guiraud & Maurin, 1992). None of those volcanic rocks have been studied in detail excepted the recent framework done on the

dolerite dyke swarms of Hama-Koussou half graben (Fagny et al. 2019) which suggest that those rocks are the results of the regional distension that occurred after the Pan African basement consolidation prior to the development of West and Central African Rift System at Late Jurassic-Early Cretaceous times. The geodynamic evolution and the timing of tectonic events leading to the occurrence of volcanic products of Cretaceous sedimentary basin of north and central Cameroon is poorly constrained. Bamwa basin in the southern north Cameroon have never been cited and remains unknown as those of Figuil, Mayo Oulo and Koum of Hama-Koussou where it is difficult to prove that the magmas were emplaced during the progressive opening of the basins excepted the later where basaltic lava flows are observed interbedded with shales (Wilson & Guiraud, 1998).

The occurrences of numerous dolerite dykes in Bamwa basin suggest that the underlined basement should have been controlled by an extensive tectonic episode or by a convergent tectonic event that may have been initiated during the early collisional phase. Systematic petrology and geochemical investigation should be carried out on Bamwa doleritic dyke swarms to evidence their petrogenesis and tectonic significance.

The main aim of this work is to provide the petrography and geochemistry features of Bamwa basin dolerites and to discuss their relevance on the geodynamic setting.

2. GEOLOGICAL SETTING

Bamwa basin basement belongs to so-called "northern pan African domain" after the subdivision of central pan African food belt chain in tree domain by Toteu (1990). This domain have been considered as the magmatic arc of Neoproterozoic overlapped on Central Adamawa-Yadé domain at 620Ma (Pouclet et al. 2006), (Penaye et al. 2006), (Isséini et al. 2012). The northern domain located west of the Tcholliré-Banyo shear zone (TBSZ, Fig. 1B) is composed of Neoproterozoic medium- to high-grade schists and gneisses, Pan-African pre-, syn-, to late-tectonic granitoids emplaced between 660 and 580 Ma and post-tectonic alkaline granitoids, which comprise mafic and felsic dykes crosscut by subcircular granites and syenites (Toteu 1990), (Toteu et al. 2004). Authors have proposed a model of continent-

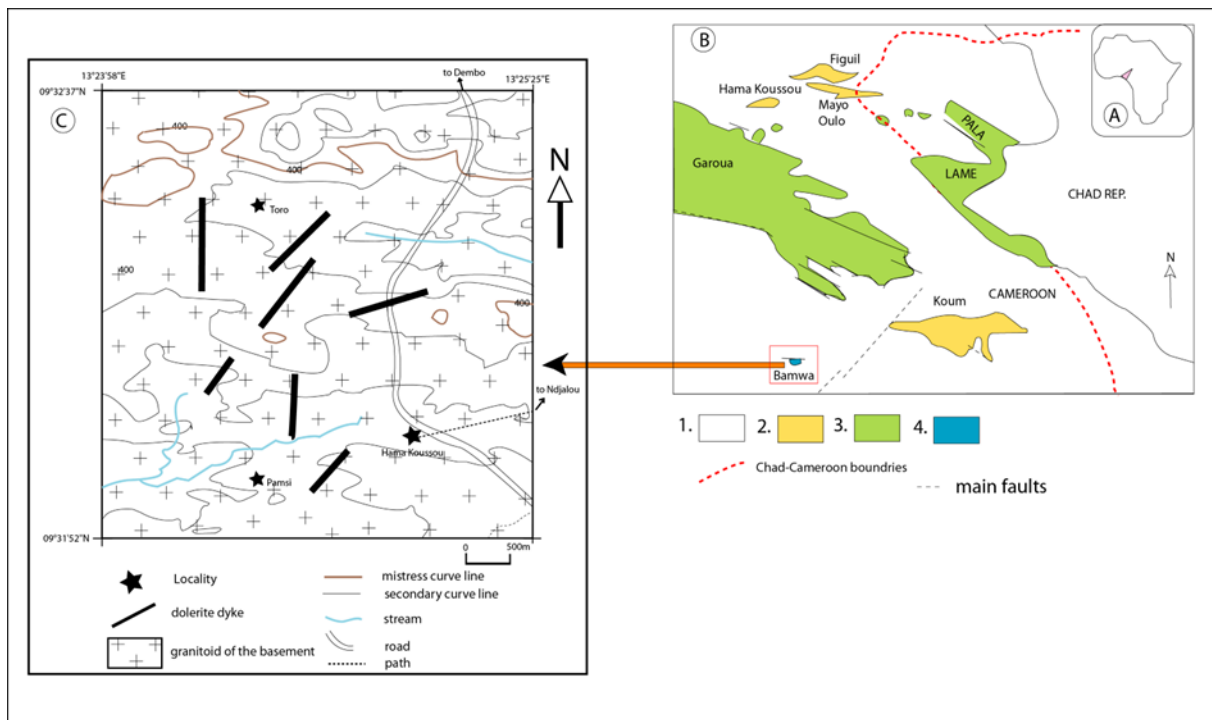


Fig. 1. (A) Location of Bamwa basin in Africa, (B) some Baremo-Aptian basins of northern Cameroon (modified after Maurin, Guiraud (1990): 1. Pan African basement; 2. Baremo Aptian basins; 3. Albo-Aptian to Cenomano-Turonian basin; 4. Bamwa basin (this study). C: Sketch map of studied area.

continent collision for the development of the central pan African belt that involved the Congo craton and the north-central Cameroon active margin (Toteu et al. 2004). The model is based on the role of the Congo craton as proved by the regional extension of external napes on its northern edge and the concomitant exhumation of the 620 Ma granulitic rocks formed at the root of the collision zone, and the late development of a strike slip fault system in central Cameroon as the result of horizontal movement following the multistage collision.

3. MATERIAL AND METHODS

Ten thin sections for petrography study have been prepared from the most representative samples of the lavas at the Laboratory of the Institute for Geological and Mining Research (IGMR) of Nkolbisson, Cameroon. Major and trace element analyses of lavas were determined using 6 representative samples (Table 1) by ICP-AES and ICP-MS at the Acme laboratory of Vancouver, Canada. The prepared sample is mixed with $\text{LiBO}_2/\text{Li}_2\text{B}_4\text{O}$ flux. Crucibles are fused in a furnace. The cooled bead is dissolved in ACS-grade nitric acid and analysed by ICP and/or ICP-MS. Loss on ignition (L.O.I.) is determined by igniting a sample split then measuring the weight loss. The geochemical data used in this work and depicted in various figures have been recalculated to 100 % on a L.O.I.-free with all Fe expressed as FeO^* .

Table 1. Bamwa basin dykes coordinates, direction, wide and length (see Fig. 1).

| Sample | Location | Latitude | Longitude | Direction | Wide (m) | Extension (m) |
|--------|-------------|-----------|------------|-----------|----------|---------------|
| FII | Bamwa basin | N08°3'20" | E13°35'56" | N77E | 4 | 450 |
| FIII | | N08°3'18" | E13°35'47" | N83E | 3-12 | 480 |
| FV | | N08°3'13" | 13°35'43" | N110E | 3 | 465 |
| FI | | 08°03'38" | 013°35'46" | N156E | 4-26 | 500 |
| FIV | | 08°03'16" | 013°35'43" | N40E | 40 | 323 |
| FVI | | 08°03'00" | 013°36'16" | N120E | 7-20 | 410 |

4. RESULTS

4.1. Field work

Dykes swarms of Bamwa basin exceptionally occurred as well exposed dykes vertically overhanging the local granitoids of the basement on 2 m (Fig. 2A) or more (Fig. 2B). Studied rocks are composed of 20 to 25 individual dykes of 1 to 26 m wide extending on 400 to 500 m before disappearing into the basement. The dolerite dykes and the granitoids exhibit the sharp contact (Fig. 2C) though the thin (0.5 to 1 cm) whitish material appears at the edge of the granitoids along the boundary. Apophyse structures of finger-like feature sometimes propagate into the basement rocks. The main trending direction of Bamwa dykes is N155E as shown in Figure 2E. Detached blocks with rough surface are scattered around the dyke and are 20 cm to 1.2 m in size. All samples display a fine- to medium-grained intergranular and show green-blackish matrix coated by 0.5 to 1 cm thick whitish patina. Freshest specimens are composed of up to 3 mm whitish plagioclase, 1 to 1.5 mm black clinopyroxene or oxides dominating the darkness groundmass (Fig. 2D). 2-5 cm enclaves of crustal origin have been found in some blocs.

4.2. Petrography

Microscope observations carried out on Bamwa dolerite have revealed various textures, from ophitic (Fig. 3A) and sub-ophitic (Fig. 3B and C) to classical dolerite (Fig. 3D and 3E) and microlitic porphyritic (Fig. 3F). All dolerites are composed of plagioclase, oxides, clinopyroxene and rare apatite crystals. In some sample, clinopyroxene are replaced by chlorite or green amphibole. Plagioclase phases are the most abundant phases (35-45 vol. %) and constitute the weft of ophitic and sub-ophitic dolerites textures (Fig. 3A and 3B). They are large (2 to 4 mm) and show prismatic shape and euhedral habit with inclusion of oxides microcrysts. Euhedral plagioclase crystals occur in some samples (Fig. 3E and 3F) as abundant microphenocrysts (Fig. 3C). Plagioclase microliths show skeletal features and regularly rimmed with oxides microcrysts in the matrix. The common sign of plagioclase crystals is their alteration feature. They are mostly clouded and show light grey to weak greenish color in rims (Fig. 3C, 3E and 3D). Larger grains show elongate prismatic habits (Figure 3E). Alteration marks like saussuritization and sericitization are also observed in some plagioclase grains. Oxides crystals are the second most abundant phases (25 to 35 vol. %) and show needle-shaped in dolerites of ophitic and sub-ophitic textures (Fig. 3A, 3B and 3C). Those of square or triangular-shaped occur in dolerites of classical dolerite to microlitic porphyritic textures (Fig. 3D, 3E and 3F). Oxides microcrysts are frequently

included in phenocrysts or lodged in their rims. Clinopyroxene phenocrysts (2 to 5 vol.%) show euhedral and skeletal shape while their microliths (3 to 7 vol.%) are acicular and should produce oxides phases through alteration process (Fig. 3A, 3B, 3C, 3D, 3E and 3F).

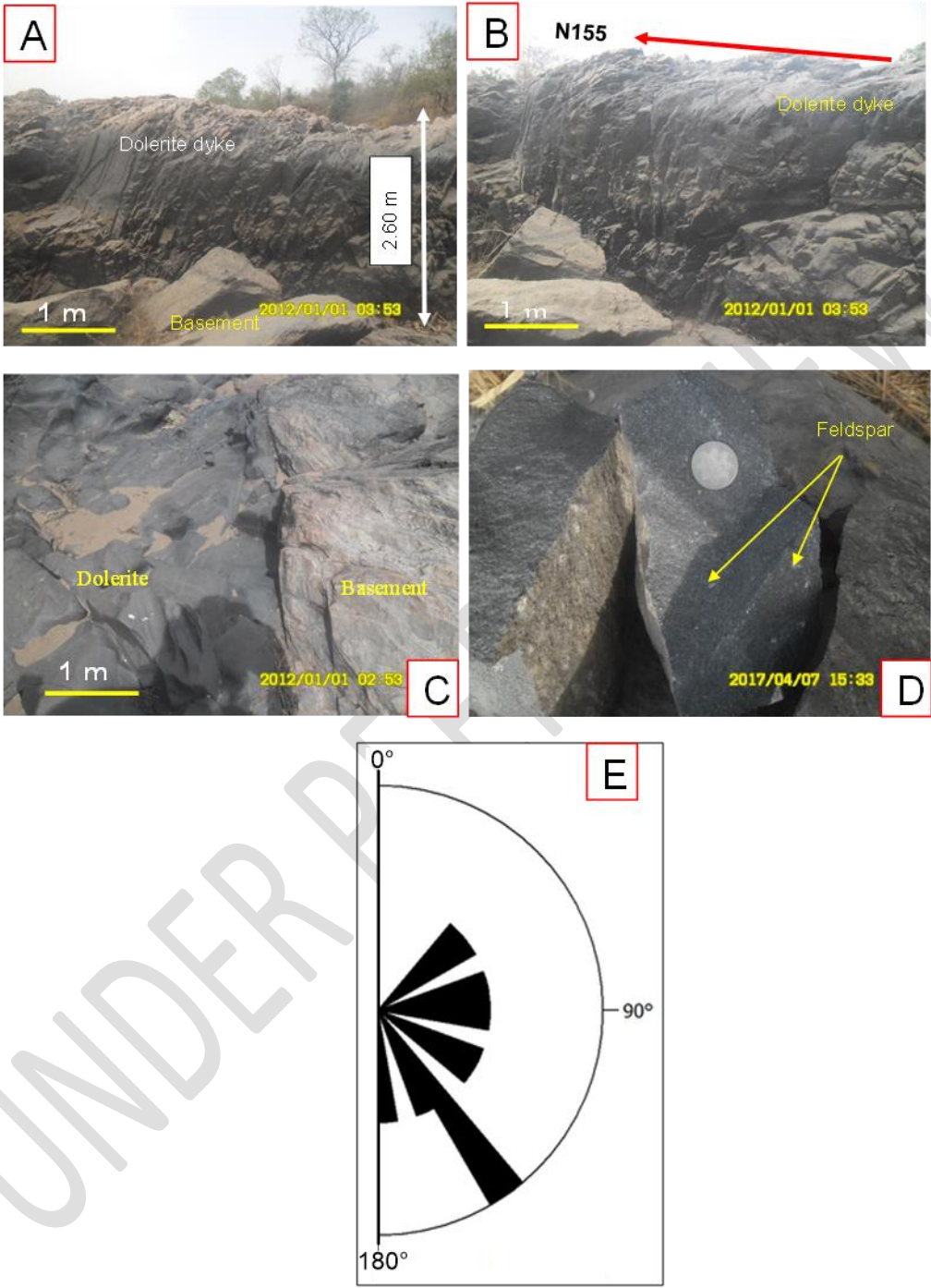


Fig. 2 Field work illustrations of Bamwa dolerite dykes. Well exposed dyke above the basement (A) along N155E trending direction (B). Dolerite-crustal contact (C) and dark hand specimen of representative samples (D) and (E) rose diagram of main trending directions of studied dykes

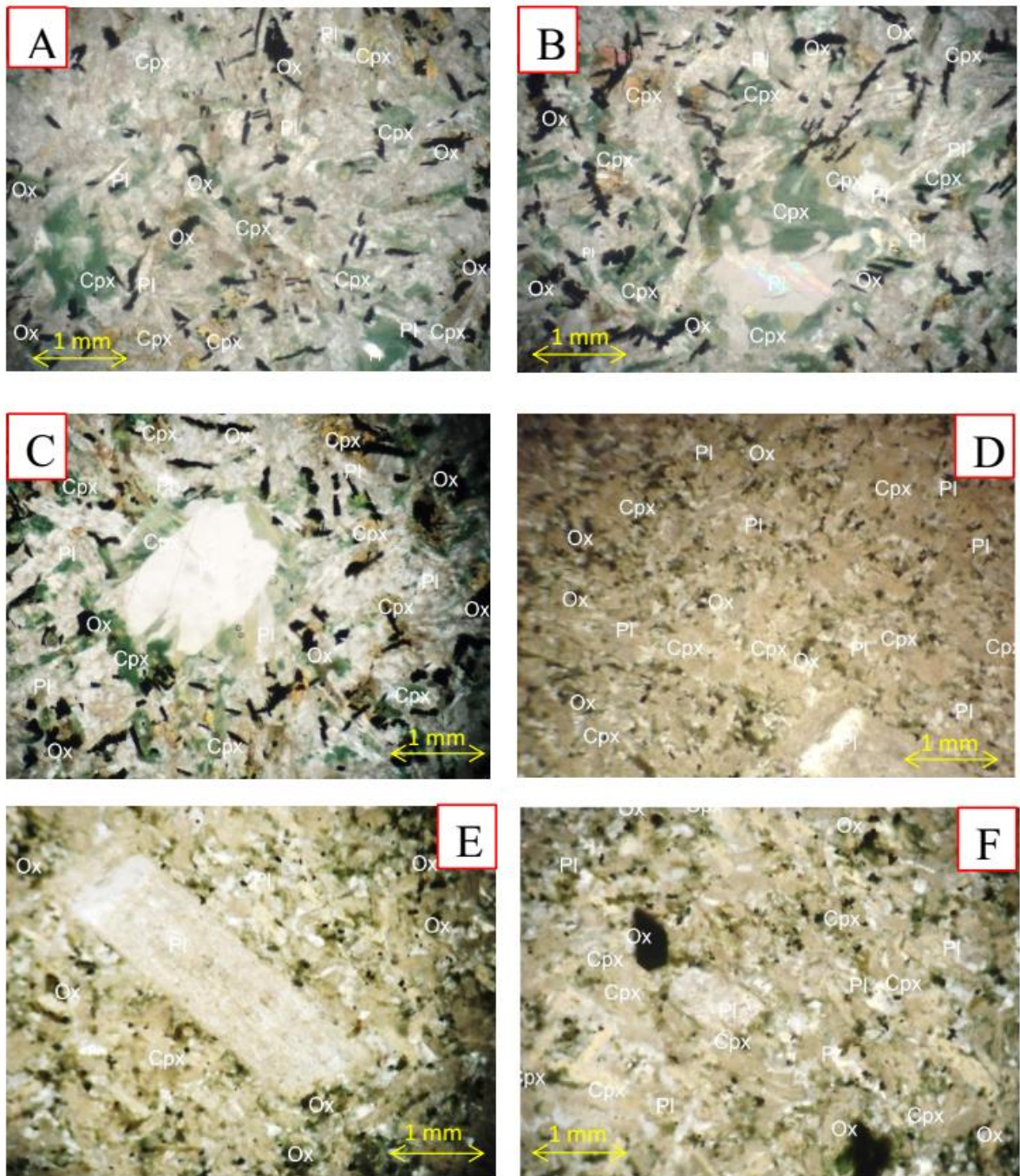


Fig. 3. Main Bamwa dolerite textures of ophitic (A) and sub-ophitic (B and C) to classical dolerite (D and E) and microlitic porphyritic (F). All containing clouded and dusted plagioclase and altered clinopyroxene crystals

4.3. Geochemistry

Representative geochemical analyses carried out on Bamwa dolerites are shown in table 2. Bamwa dolerites have been distinguished as basaltic trachyandesite (FI, FIII, and FVI), andesite (FII), dacite (FV) and rhyolite ((FV), Fig. 4) according to IUGS (International Union of Geological Sciences) TAS (Total Alkali Silica, $\text{Na}_2\text{O} + \text{K}_2\text{O}$) vs. SiO_2 diagram, L.O.I. free recalculated (after Le Maître, 2002). In raw geochemical analyzed data, some samples (andesite, dacite and rhyolite) have low (< 2 wt. %) low

L.O.I. contents. Calculated Mg# ($Mg\# = 100 * (MgO/40.32) / (MgO/40.32 + FeOt/71.85)$) using MgO and FeOt contents of identified lavas give 36.62 to 73.07 for trachyandesite, 51.07 for andesite, 45.04 and 3.65 for dacite and rhyolite, respectively. Geochemical data show wide range of oxides variation from

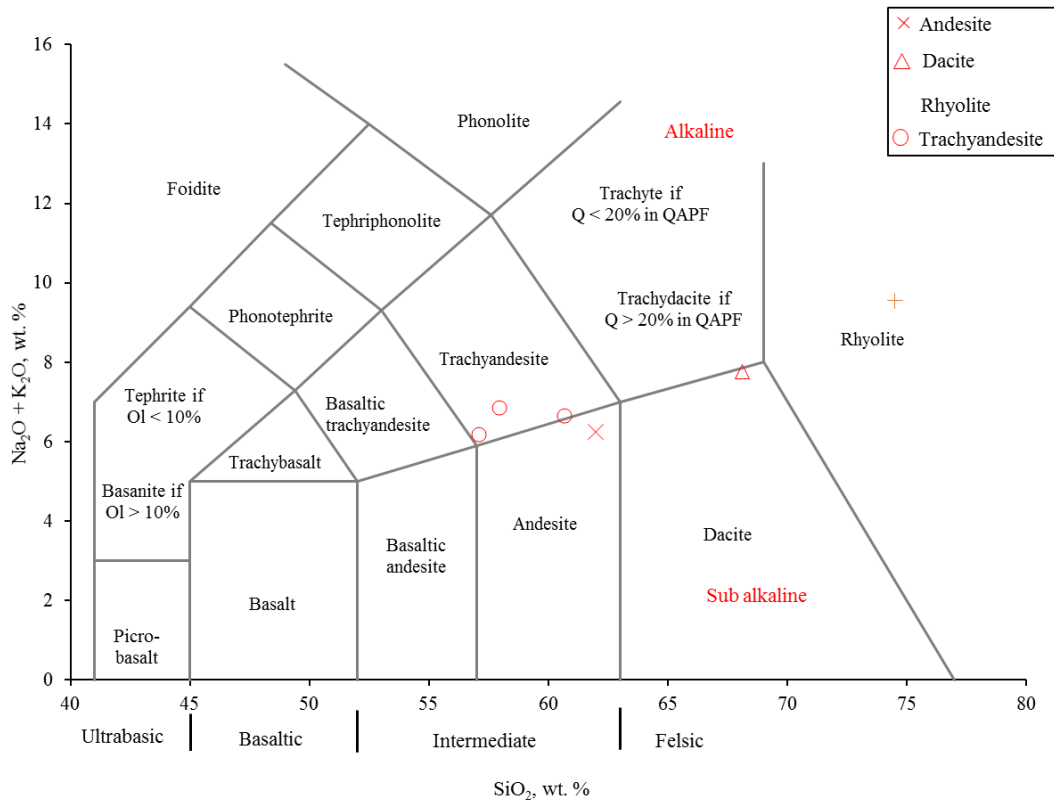


Fig. 4. ($Na_2O + K_2O$) vs. SiO_2 diagram after L.O.I. free recalculated (after Le Maitre, 2002) of Bamwa dolerites. Dashed line between alkaline and sub alkaline fields according to Miyashiro (1978).

SiO_2 content (57.06 to 74.50 wt. %), TiO_2 (0.11 to 1.45 wt. %), Al_2O_3 (12.85 to 17.70 wt. %), Fe_2O_3 (2.36 to 7.64 wt. %), MgO (0.05 to 8.09 wt. %), CaO (0.53 to 6.41 wt. %), Alkali (Na_2O+K_2O : 6.18 to 9.56 wt. %) to P_2O_5 (0.01 to 0.31 wt. %). Low contents of major elements are found in rhyolite lava excepted SiO_2 and alkali which are high in rhyolite and low in basaltic trachyandesite.

Transitional element contents of Bamwa dolerites generally decrease from basaltic trachyandesite to rhyolite (Ni: 295 to < 20 ppm, Sc: 15 to 1 ppm, Co: 25.2 to <0.2 ppm, V: 152 ppm in andesite to < 8 ppm in rhyolite, Cu: 28 to < 5 ppm) with high content found in trachyandesite FIII and andesite FII excepted Zn which content decrease from to trachyandesite to dacite and become high in rhyolite (159 ppm).

Incompatible trace element contents show wide variations. Alkali and alkali earth elements Rb, Ba, Sr show contrasting compositional variations. Ba contents are high and increase from trachyandesite to dacite with very low contents in rhyolite (8 ppm). High Rb contents are found in rhyolite (301.9 ppm) and low contents are found in andesite (37.6 ppm) whereas Sr contents decrease from trachyandesite (700.0 to 12.2 ppm) in rhyolite with high value in andesite (759.5 ppm). Rb/Sr ratios are low in all lavas (< 1) excepted rhyolite (24.75). High Field Strength Elements (HFSE) vary in the same

way with very low contents of Nb and Ta in all lavas. Relatively high contents of those elements are found in rhyolite (78.4 and 5.5 ppm, respectively). Nb/Ta ratios are relatively constant (12.2-14.3). High value of Nb/Ta (18.1) is found in trachyandesite FVI. Ba/Nb ratios show contrast variation:

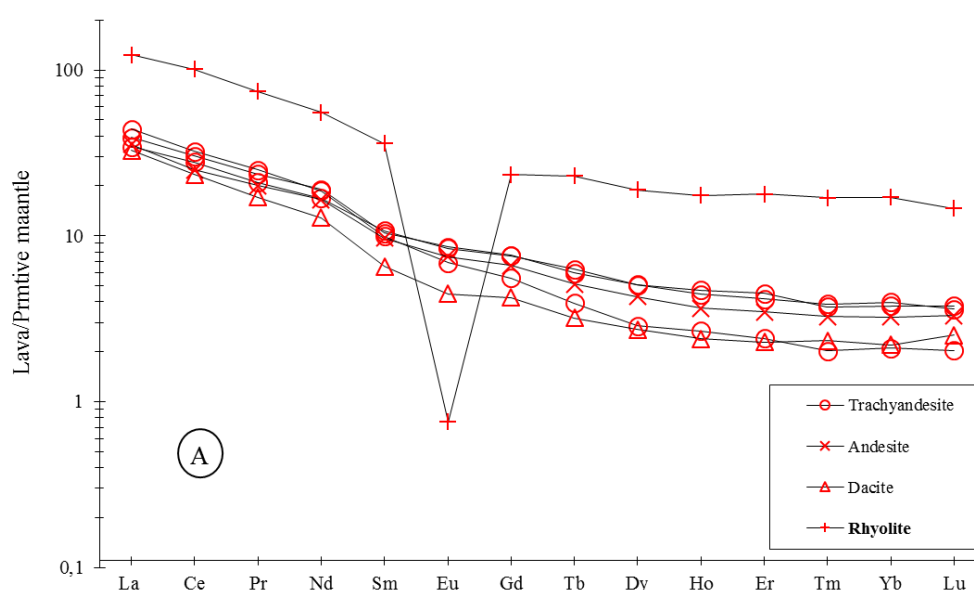
Table 2. ICP-AES and ICP-MS geochemical analyses of Bamwa dolerites

UNDER PEER REVIEW

| Lava | Trachyandesite | | | Andesite | Dacite | Rhyolite |
|--------------------------------|----------------|--------|--------|----------|--------|----------|
| sample | FVI | FI | FIII | FII | FV | FIV |
| SiO ₂ (wt %) | 57.06 | 57.95 | 60.64 | 61.97 | 68.11 | 74.50 |
| TiO ₂ | 1.36 | 1.45 | 0.70 | 1.16 | 0.49 | 0.11 |
| Al ₂ O ₃ | 16.92 | 17.70 | 13.08 | 15.32 | 15.69 | 12.85 |
| Fe ₂ O ₃ | 7.62 | 7.64 | 5.32 | 6.24 | 3.28 | 2.36 |
| MnO | 0.11 | 0.10 | 0.08 | 0.08 | 0.05 | 0.03 |
| MgO | 4.05 | 2.48 | 8.09 | 3.66 | 1.51 | 0.05 |
| CaO | 6.41 | 5.50 | 5.23 | 5.06 | 3.01 | 0.53 |
| Na ₂ O | 3.96 | 4.57 | 3.09 | 4.27 | 4.87 | 4.83 |
| K ₂ O | 2.22 | 2.30 | 3.57 | 1.99 | 2.88 | 4.72 |
| P ₂ O ₅ | 0.28 | 0.31 | 0.20 | 0.26 | 0.12 | 0.01 |
| Sum | 100.00 | 100.00 | 100.00 | 100.00 | 100.00 | 100.00 |
| Ba (ppm) | 609 | 502 | 735 | 641 | 786 | 8 |
| Sc | 14 | 11 | 12 | 11 | 5 | 1 |
| Be | 1 | 5 | 4 | 1 | 1 | 9 |
| Ni | 49 | <20 | 295 | 61 | <20 | <20 |
| Cr | | | | | | |
| Co | 25.2 | 19.2 | 25.2 | 18.6 | 8.3 | <0.2 |
| V | 136 | 122 | 86 | 152 | 44 | <8 |
| Cs | 0.6 | 1.6 | 1.0 | 0.9 | 0.9 | 2.5 |
| Cu | 28 | 25 | 6 | 24 | 11 | <5 |
| Hf | 4.3 | 4.3 | 4.5 | 3.8 | 3.8 | 26.6 |
| Nb | 16.3 | 13.8 | 7.7 | 9.7 | 9.2 | 78.4 |
| Rb | 63.6 | 59.2 | 89.1 | 37.6 | 64.9 | 301.9 |
| Sr | 700.0 | 506.7 | 420.9 | 759.5 | 577.6 | 12.2 |
| Ta | 0.9 | 1.0 | 0.6 | 0.7 | 0.7 | 5.5 |
| Th | 5.4 | 3.2 | 14.5 | 3.4 | 6.4 | 50.1 |
| U | 1.6 | 1.0 | 4.7 | 1.4 | 1.9 | 6.6 |
| W | 0.6 | 0.8 | 0.9 | 0.6 | 0.8 | <0.5 |
| Zn | 71 | 77 | 63 | 66 | 47 | 159 |
| Zr | 173.60 | 169.30 | 168.90 | 145.80 | 142.60 | 777.50 |
| Y | 16.60 | 16.20 | 9.20 | 12.80 | 8.90 | 68.10 |
| La | 24.10 | 21.10 | 27.10 | 21.80 | 20.10 | 75.70 |
| Ce | 48.50 | 44.60 | 51.90 | 40.00 | 37.60 | 162.20 |
| Pr | 5.69 | 5.09 | 6.03 | 4.84 | 4.13 | 17.96 |
| Nd | 22.6 | 20.0 | 22.2 | 19.7 | 15.3 | 66.0 |
| Sm | 4.01 | 4.14 | 3.85 | 3.74 | 2.52 | 13.90 |
| Eu | 1.25 | 1.22 | 1.00 | 1.09 | 0.65 | 0.11 |
| Gd | 3.91 | 3.89 | 2.86 | 3.39 | 2.18 | 11.97 |
| Tb | 0.56 | 0.59 | 0.37 | 0.48 | 0.30 | 2.16 |
| Dy | 3.22 | 3.24 | 1.83 | 2.75 | 1.74 | 12.05 |
| Ho | 0.63 | 0.67 | 0.38 | 0.52 | 0.34 | 2.49 |
| Er | 1.74 | 1.87 | 1.00 | 1.45 | 0.95 | 7.43 |
| Tm | 0.25 | 0.24 | 0.13 | 0.21 | 0.15 | 1.09 |
| Yb | 1.65 | 1.57 | 0.87 | 1.34 | 0.91 | 7.07 |

| | | | | | | |
|----|------|------|-------|------|------|-------|
| Lu | 0.23 | 0.24 | 0.13 | 0.21 | 0.16 | 0.93 |
| Pb | 5.00 | 3.10 | 10.50 | 3.10 | 6.20 | 24.40 |

Trachyandesite (36.4-95.5), andesite (61.1), dacite (85.4) and rhyolite (0.1). Hf contents are low and relatively constant (3.8-4.5 ppm) with high contents in rhyolite (26.6 ppm). Zr contents vary in the same way but are relatively high in all lavas. The highest Zr content is observed in rhyolite (777.5 ppm). Values of Zr/Hf ratios are relatively constant in all lavas (37.5-40.4) but remain low in rhyolite (29.2). Values of Zr/Nb ratios are < 20 for all lavas excepted the slight high value (21.9) of trachyandesite FIII. Th contents are low (< 7 ppm) and also show contrasting values between lavas. Relatively high contents of Th are observed in trachyandesite FIII (14.5 ppm) and rhyolite (50.1). Y contents are low and highest values characterized rhyolite lava (68.1 ppm) for relatively constant Y/Nb ratios (1.0-1.3). Low Y/Nb value is also observed in rhyolite (0.9). Values of Y/Rb ratios are low (< 0.5) and the lowest values are found in trachyandesite FIII, dacite FV and the mean value characterizes rhyolite lava (0.2). REE patterns (Fig. 5A) of Bamwa dolerites (normalization after McDonough and Sun, 1995) show a regular decrease from high LREE (10-50 times) to low HREE (3-4 times) the mantle values. A weak negative Eu anomaly is observed in those patterns whereas the pronounced negative anomaly in this element is shown by rhyolite pattern. Values of Cen/Ybn ratios are relatively low (5.9-7.6) for some lavas excepted trachyandesite FIII (Cen/Ybn=15.4) and dacite (Cen/Ybn=10.6) where those values are relatively high. Primitive mantle-normalized multi-elements patterns of Bamwa dolerites (Fig. 5B) generally show decreased values from incompatible to compatible elements. Rhyolite patterns marked-down from others lavas. From trachyandesite to dacite, patterns show negative anomalies in Th (excepted trachyandesite FIII), Nb, Ta, P and Ti while positive anomalies are observed in K and Zr. Pronounced negative anomalies are observed for rhyolite in Ba, P, Sr, Ti and Eu and positive anomalies in Rb, Th, Hf and Zr.



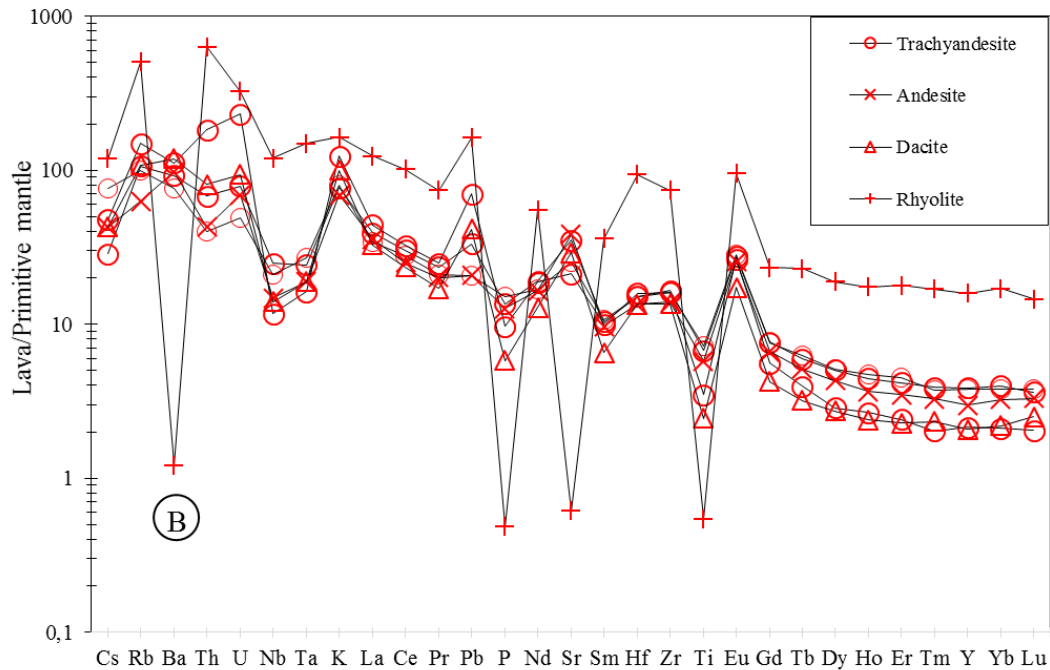


Fig. 5. Primitive mantle normalized REE (A) and trace (B) diagrams (after McDonough and Sun, 1995) of Bamwa dolerites.

5. DISCUSSIONS

On the basis of detailed field work, studied dolerites occur in N155E trend, which corresponds to the main Pan African faults directions (Moreau et al. 1987), leading to emplacement of Bamwa dolerites during the Pan African crustal consolidation (Cornachia and Dars, 1983; Benkhelil et al. 1998). Bamwa dolerites thus may be considered as the records of stress conditions, feeding weak crustal cracks of the Pan African mobile zones (Fagny et al. 2019). The widths of the dykes vary from a few meters to over 50 m, features exhibiting by “giant dykes” after Scott and Ernst (2008), which apophyse features indicate that studied dykes were emplaced along preexisting fractures.

Bamwa basin dolerites exhibit the geochemical characters of continental tholeiites (Fig. 6) of low TiO_2 composition ($\text{TiO}_2 < 2$ wt. %). This suggestion is ascertained by Nb, Ta and Ti anomalies (Dupuy and Dostal, 1984) shown on spider diagram (Fig. 5B). Some lavas fall out of the continental tholeiites field probably because they have experienced others magmatic processes effects. Relatively low values of Y/Nb ratios contrast with the continental tholeiites feature of studied dolerites for the same reason as in certain conditions, immobile elements as Nb and Zr can be affected (Hellman et al. 1979; Hynes, 1980). Relatively constant values of Zr/Hf and Nb/Ta ratios attest the co-genetic character of studied lavas (Table 3).

5.1. Magma source

Mantle source characteristic of Bamwa dolerites are constrained through values of trace element ratios. $(\text{La}/\text{Ce})_n$ and Zr/Nb of studied dolerites are respectively > 1 and < 20 , indicating enriched mantle source (Marcelot et al. 1989; Sun and McDonough, 1989; Morata et al. 1997; [Muhammad et al. 2019](#))

for Bamwa dolerites (Table 3). Nb, Ta and Ti anomalies observed on spider diagrams of Bamwa dolerites are usually considered

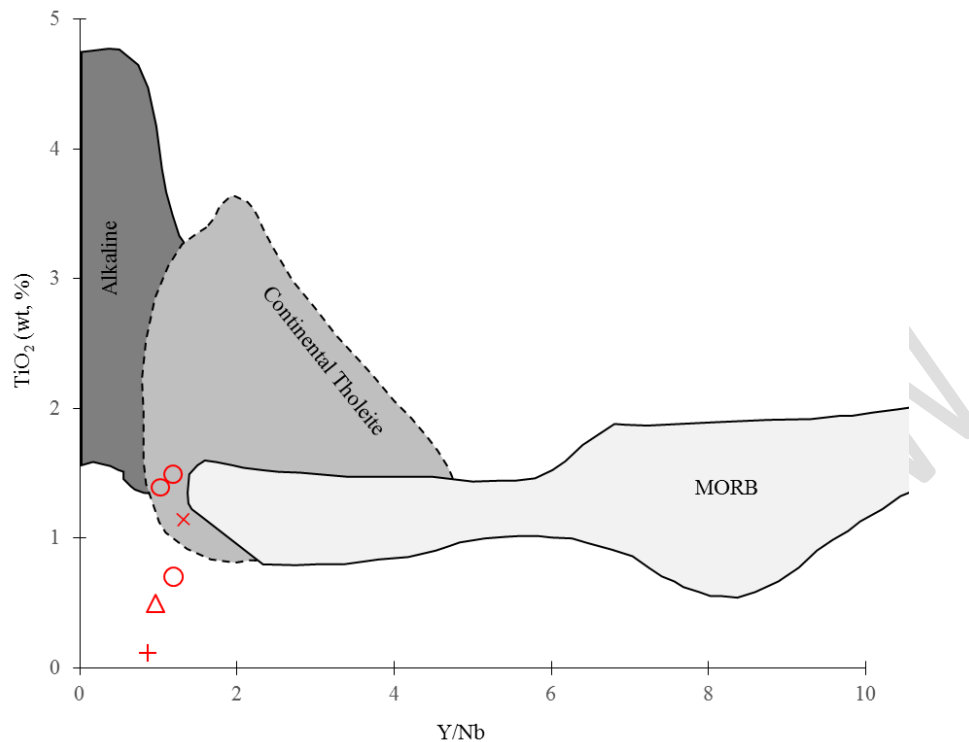


Fig. 6. Composition of Bamwa dolerites plotted in TiO₂ vs Y/Nb diagram after Floyd and Winchester (1975). Same Symbols as Fig. 5.

as continental tholeiites features (Dupuy et Dostal, 1984). Although these patterns show the enriched LREE and incompatible elements of studied lavas, Nb, Ta and Ti anomalies are the strong contrast with OIB or MORB mantle sources. They are usually considered to reflect an enriched sub-continental lithospheric mantle (SCLM) source which have undergone metasomatism process during subduction (Puffer, 2003; Cebria et al. 2003; Deckart et al. 2005; Marzoli et al. 2018; Muhammad et al. 2019). The plots of the dolerite rocks of study area mostly fall in the fields of SCLM of La/Ba versus La/Nb diagram (Fig. 7). High values of La/Nb > 2 and relatively low values of La/Ba > 2 strongly argue for SCLM as the best candidate to be pointed out as mantle source of studied dolerites. Low values of (Tb/Yb)_n ratios (1.3-1.8) suggest the shallow mantle source of spinel stability field (Wang et al. 2002). Trachyandesite FI, FVI and rhyolite FIV have the values of La/Nb < 2. This can be interpreted as the consequence of crustal contamination. SCLM source of studied dolerites should have undergone the high partial melting rate as suggested by relatively low values of (Ce/Yb)_n (5.9-7.7). High values of these ratios are result of metasomatism process or more the progressive crustal contamination process (Fig. 8 and 9).

5.2. Petrogenesis of Bamwa dolerites

Petrographic and geochemical studies of the dolerite dykes of Bamwa Basin have shown that studied dolerites have experienced a complex petrogenetic history. Assimilation and fractional crystallization, fluid infiltration and crustal contamination are main processes which should have controlled the petrogenesis of Bamwa basin dolerites. Low contents of transitional elements coupled

with that of Mg# of Bamwa dolerites attest their evolved characters through fractional crystallization process (Fig. 10). This hypothesis is attested by the global decreasing of major elements and the

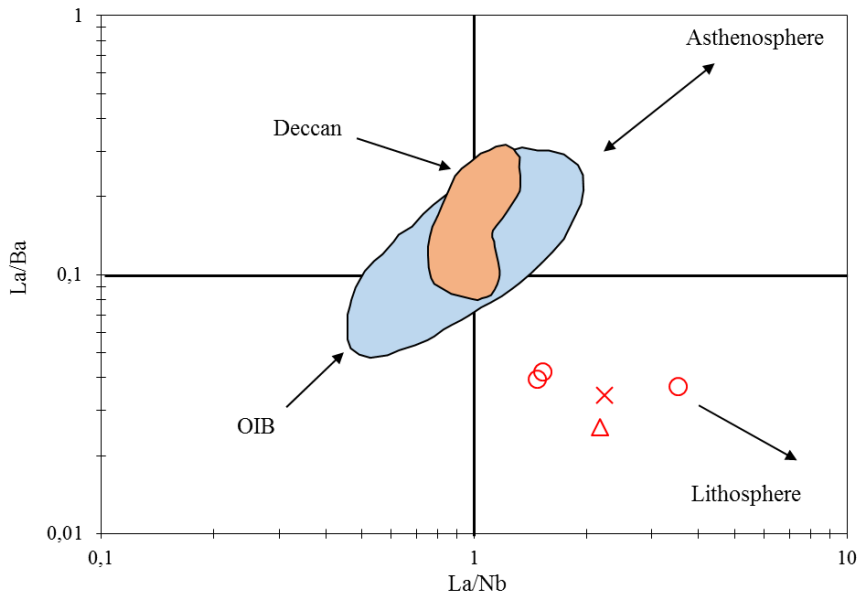


Fig. 7. La/Ba versus La/Nb diagram for Bamwa dolerites. Reference fields are from Saunders et al. (1992). Same Symbols as Fig. 5.

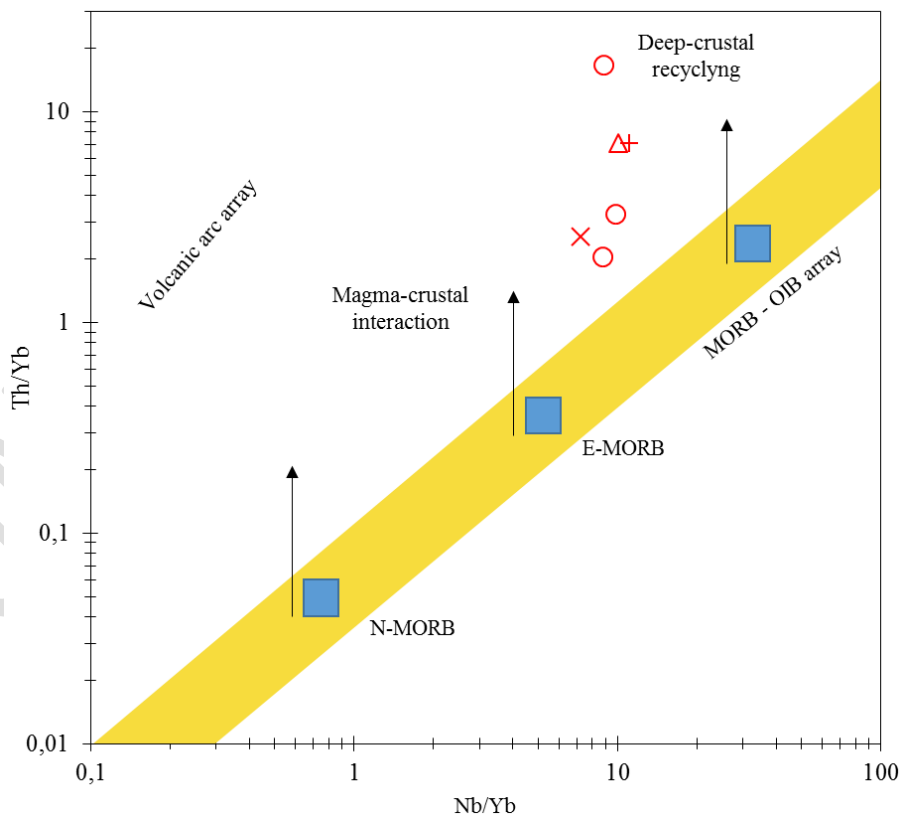


Fig. 8. Th/Yb vs Nb/Yb diagram after Pearce (2008). Bamwa dolerites plot close to the deep-crustal recycling field out of the MORB–OIB array. Same Symbols as Fig. 5.

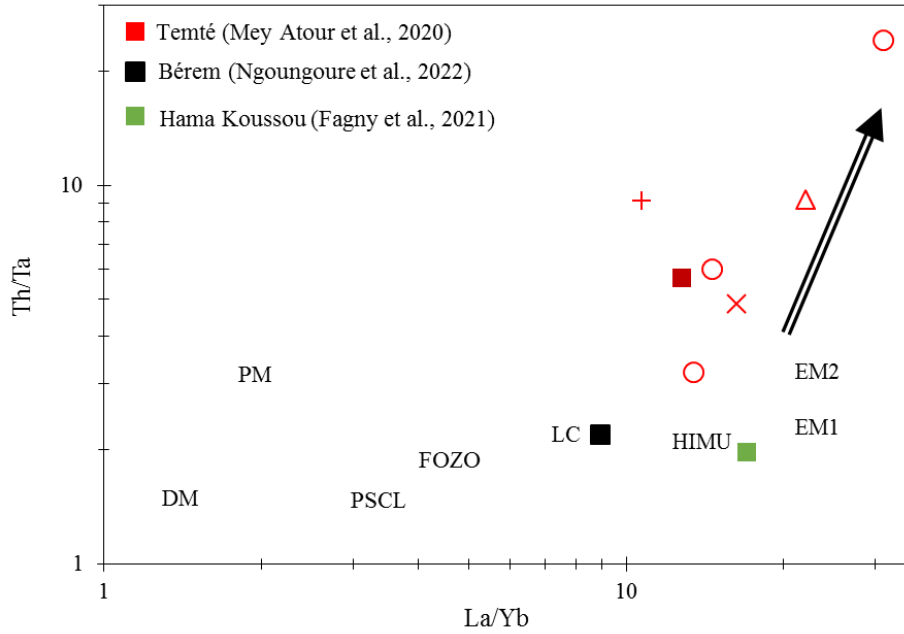


Fig. 9. Th/Ta vs La/Yb diagram of Bamwa dolerites (after Sun and McDonough, 1989) OIB, E-MORB, N and PM (Parental Magma) from Genik (1992). Continental Crust (CC) from Taylor and McLennan (1985). Same Symbols as Fig. 5.

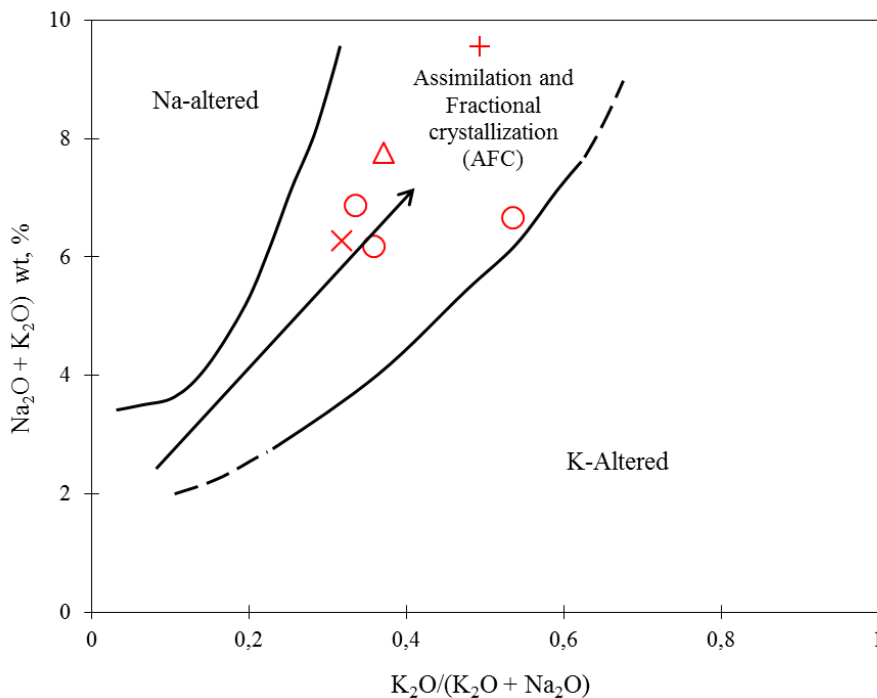


Fig. 10. Plot of Bamwa dolerites in Alk vs $K_2O / (K_2O + Na_2O)$ diagram of Hughes (1973). Same Symbols as Fig. 5.

increasing of incompatible elements contents from basaltic trachyandesite to rhyolite (Table 2). Negative anomalies on spider diagrams reinforce these observations. Involved minerals should be plagioclase, clinopyroxene, oxides, apatite or hornblende.

On petrographic view, metasomatism process should be sustained by typical alteration features of some minerals which may throw light on the possible alteration processes which have operated during the formation of Bamwa dolerites: Clouded plagioclase crystals, clinopyroxene alteration and dust aspect of some feldspar crystals, which are petrographic markers of fluid-rock interaction. These alteration signs might geochemically involve the addition of certain elements such as Rb, Ba, Th, La and K and the removal of Sc, Cr, Co, Ni, Si, Al, Fe, Mg and Ca (Sengupta et al. 2014). Raw Bamwa dolerite geochemical analyses show that LOI of all samples are <3.5 wt. % (excepted trachyandesite FI, with LOI of 4.4 wt. %), indicating that alteration signs exhibiting by studied dolerites are the results of in situ igneous process, certainly métasomatisme. It has been observed that highly variable Rb contents within a group of rocks so as that of mobile elements like Ba, Rb, Th are results of fluid-rock interaction (Backman et al. 1988). Bamwa dolerites show large variation of Rb, Ba, Th or Sr contents. Trachyandesite FIII and rhyolite FIV with high Rb contents thus stand as the most metasomatized lavas among studied dolerites. The occurrence of enclaves of crustal origin in some dolerite blocks may suggest the magma-crustal interaction for the petrogenesis of studied dolerites. This hypothesis shows that Bamwa dolerites should have been contaminated by crustal materials. Trace elements contents or values of their ratios, namely Ce/Pb and Nb/U strongly ascertain the crustal contamination process of Bamwa dolerites (Figure 11A and 11B) as their ratios are closed to those of continental crust (Ce/Pb: 4 and Nb/U: 9-12, Hofmann et al. 1986) so as Nb/Ta ratios which values of some lavas are similar to those of continental crust (12-13, Pfander et al. 2007). Relatively high values of Th/Ta (>3.6) and Ba/Zr (2-6) ratios also argue for magmatic contamination by crustal materials (Cabanis et al. 1990; Fitton et al. 1998) of studied dolerites. High values of La/Nb and La/Ta ratios distinguish the trachyandesite FIII (La/Nb: 3.52 and La/Ta: 45.17) and in certain degree the andesite FII (La/Nb: 2.25 and La/Ta: 31.14) as the most contaminated lavas, as these ratios are closed to that of continental crust (La/Nb > 1.5 and La/Ta > 30, Taylor and McLennan, 1985). The low values of those ratios (La/Nb: 0.97 and La/Ta: 13.76) and that of Ba/Zr (0.01) argue for non-contamination of rhyolite lava.

5.3. Geodynamic setting

In tectonic discrimination diagrams $Y/15-La/10-Nb/8$ (Fig. 12A) of Cabanis and Lecolle (1989) and $Th-Tbx3-Tax2$ of Cabanis and Thiéblemont (1988), the plots of studied dolerites mostly fall in the fields of late to post orogenic domains and volcanic arc basalt respectively, suggesting a possible arc-back arc setting for Bamwa dolerites. Bamwa dolerites show high and variable Th/La at low and nearly constant Sm/La ratios (Table 3), similar to basalts from enriched mantle sources additionally with variable amounts (10 to 50 %) of crustal material or subducted sediments (Plank, 2005). These observations suggest the possible occurrence of studied dolerites in the subduction tectonic setting. Well-pronounced Nb-Ta and P negative anomalies similar to global subducting sediment (Plank, 2005) are strong arguments in favor for Bamwa dolerites to be considered as fingerprints of post subduction magmatic events. U-Pb age of 599 ± 9 Ma of mafic dykes of Poli group, 100 km North of Bamwa basin is interpreted as the age of mafic magma emplacement (Toteu et al. 2022), i.e. syn to post Pan African.

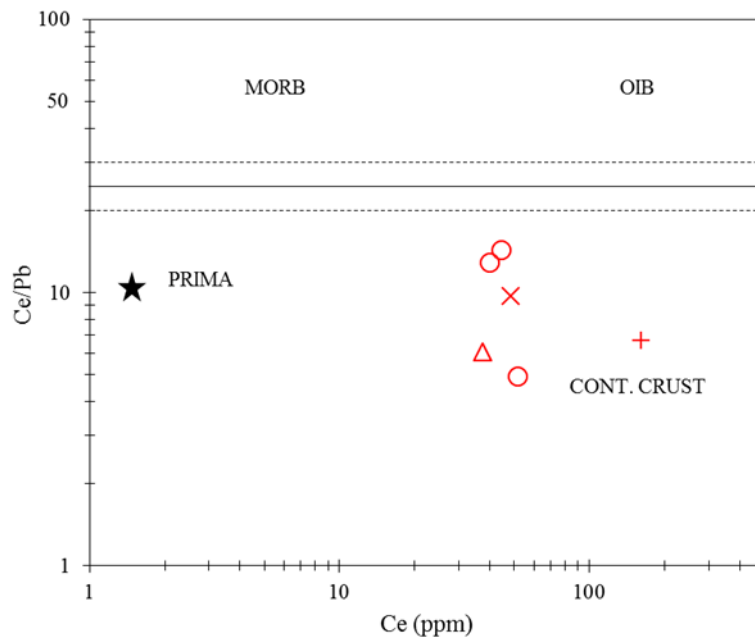
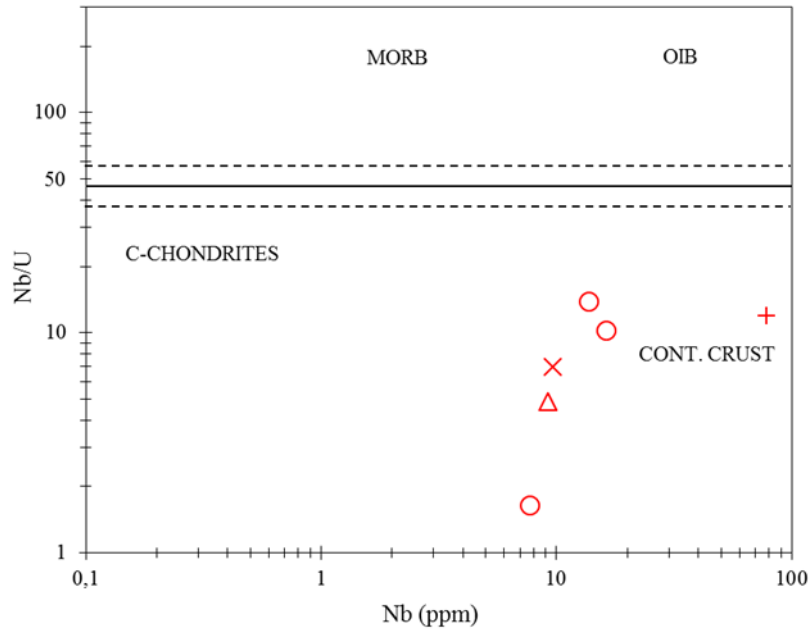


Fig. 11. Nb/U vs Nb (ppm) for Bamwa dolerites closed to continental crust field (after Hofmann et al. 1986). Same Symbols as Fig. 5.

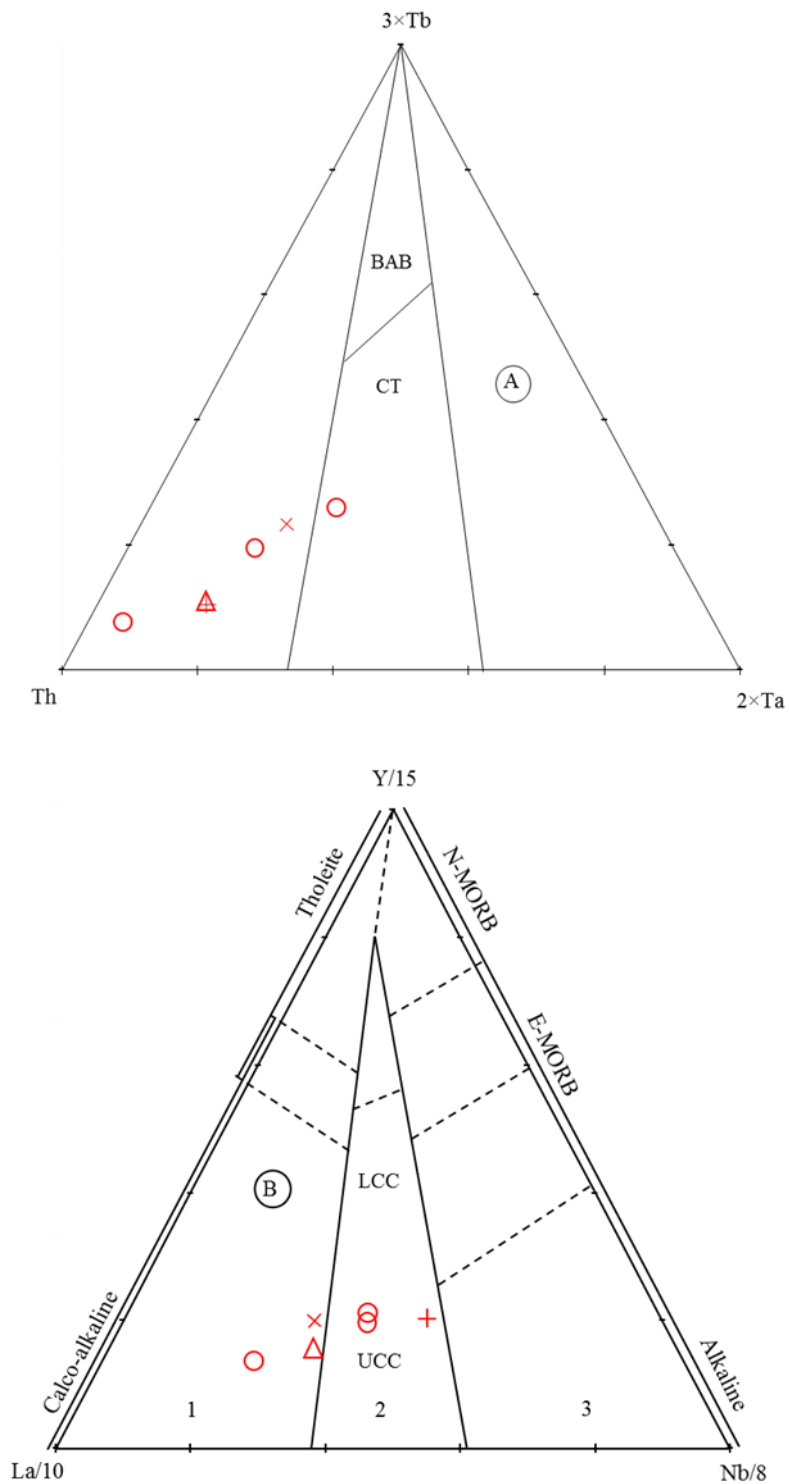


Fig. 12. Composition of Bamwa dolerites plotted in (A) (Th-3Tb-2Ta) triangle after Cabanis and Thiéblemont (1988), BAB: Back-Arc Basin Basalts, CT: Continental Tholeiites; 1. Orogenic Basalts, 2. Continental Tholeiites and Arc Basin Basalts and orogenic Basalts. (B) Y-La-Nb (after Cabanis and Lecolle, 1989), CC: Continental Crust (mean value), LCC: Lower Continental Crust, UCC: Upper Continental Crust; 1. Arc-related orogenic series, 2. Intermediate domain of continental tholeiites and 3 Anorogenic series of oceanic ridges and intraplate alkaline basalts. Same Symbols as Fig. 5.

Table 3. Main values of trace element ratios of Bamwa dolerites.

| Lava | Trachyandesite | | | Andesite | Dacite | Rhyolite |
|--------|----------------|-------|-------|----------|--------|----------|
| Th/Ta | 3.20 | 6.00 | 24.17 | 4.86 | 9.14 | 9.11 |
| Y/Nb | 1.17 | 1.02 | 1.19 | 1.32 | 0.97 | 0.87 |
| Nb/Ta | 13.80 | 18.11 | 12.83 | 13.86 | 13.14 | 14.25 |
| Zr/Hf | 39.37 | 40.37 | 37.53 | 38.37 | 37.53 | 29.23 |
| Th/La | 0.15 | 0.22 | 0.54 | 0.16 | 0.32 | 0.66 |
| Sm/La | 0.20 | 0.17 | 0.14 | 0.17 | 0.13 | 0.18 |
| Rb/Sr | 0.12 | 0.09 | 0.21 | 0.05 | 0.11 | 24.75 |
| Ba/Zr | 2.97 | 3.51 | 4.35 | 4.40 | 5.51 | 0.01 |
| Nb/U | 13.80 | 10.19 | 1.64 | 6.93 | 4.84 | 11.88 |
| Ce/Pb | 14.39 | 9.70 | 4.94 | 12.90 | 6.06 | 6.65 |
| Zr/Nb | 12.27 | 10.65 | 21.94 | 15.03 | 15.50 | 9.92 |
| La/Nb | 1.53 | 1.48 | 3.52 | 2.25 | 2.18 | 0.97 |
| La/Ta | 21.10 | 26.78 | 45.17 | 31.14 | 28.71 | 13.76 |
| La/Nb | 1.53 | 1.48 | 3.52 | 2.25 | 2.18 | 0.97 |
| Ce/Ybn | 7.35 | 7.61 | 15.44 | 7.73 | 10.69 | 5.94 |
| Tb/Ybn | 1.66 | 1.50 | 1.87 | 1.58 | 1.45 | 1.35 |
| La/Cen | 1.23 | 1.30 | 1.36 | 1.42 | 1.39 | 1.22 |

6. CONCLUSION

Well exposed dykes swarms of doleritic composition overhang vertically the locale granitoids basement of Bamwa basin of the north Cameroon along N155E. Dykes are 1 to 26 m wide and extending on 400 to 500 m. They display a fine- to medium-grained intergranular and show green-blackish matrix of sub-ophitic, classical dolerite and microlitic porphyritic textures. All samples contain clouded plagioclase, oxides, clinopyroxene, apatite, chlorite and amphibole crystals. Bamwa dolerites are distinguished as basaltic trachyandesite, andesite, dacite and rhyolite. They are results of high partial melting rate of lithospheric mantle source. Bamwa dolerites are fingerprints of post Pan African subduction magmatic events. Studied dolerites have experienced a complex petrogenetic history through assimilation and fractional crystallization, fluid infiltration and varying degrees of crustal contamination processes during ascent and emplacement.

Disclaimer (Artificial intelligence)

Option 1:

Author(s) hereby declare that NO generative AI technologies such as Large Language Models (ChatGPT, COPILOT, etc.) and text-to-image generators have been used during the writing or editing of this manuscript.

8. REFERENCES

- Backman, J., Duncan, R. A., et al. (1988). *Ocean Drilling Program Scientific Results*, 115: College Station, TX. [doi:10.2973/odp.proc.ir.115.1988](https://doi.org/10.2973/odp.proc.ir.115.1988)
- Ben khelil, J., Mascle, J., Guiraud, M. (1998) Sedimentary and structural characteristics of the cretaceous along the Côte d'Ivoire Ghana transform margin and in the Benue trough: A comparison. In Mascle, J., Lohmann, G.P., and Moullade, M. (Eds.). *Ocean Drilling Program Scientific Results* 159. <https://doi.org/10.2973/odp.proc.sr.159.007.1998>
- Cabanis, B., Thiéblemont, D. (1988) La discrimination des tholéiites continentales et des basaltes arrière-arc. Proposition d'un nouveau diagramme Th-Tbx3-Tax2. *Bulletin de la Société géologique de France*, 8 (IV, 6), 927-935. <https://doi.org/10.2113/gssgfbull.IV.6.927>
- Cabanis, B., Lecolle, M. (1989). Le diagramme La/10-Y/15-Nb/8 : un outil pour la discrimination des séries volcaniques et la mise en évidence des processus de mélange et/ou de contamination crustale. *Comptes rendus de l'Académie des sciences*, 309 (2), 2023-2029.
- Cebria, JM, Lopez-Ruiz, J., Doblas, M., Martins, LT., Munha, J. (2003). Geochemistry of the early Jurassic Messejana-Plasencia dyke (Portugal-Spain); implications on the origin of the Central Atlantic Magmatic Province. *Journal of Petrology*, 44, 547-568. <https://doi.org/10.1093/petrology/44.3.547>
- Cornacchia, M., Dars, R. (1983). Un trait structural majeur du continent Africain. Les linéaments Centrafricains, du Cameroun au Golfe d'Aden. *Bulletin de la Société géologique de France*, 7 (XXV):1 :101-109. <https://doi.org/10.2113/gssgfbull.S7-XXV.1.101>
- Deckart, K., Bertrand, H., Liegeois, JP. (2005). Geochemistry and Sr, Nd, Pb isotopic composition of the Central Atlantic Magmatic Province (CAMP) in Guyana and Guinea. *Lithos*, 82, 282-314. <https://doi.org/10.1016/j.lithos.2004.09.023>
- Marzoli, A., Callegaro, S., Dal Corso, J., Davies, JHFL., Chiaradia, M., et al. (2018). The Central Atlantic Magmatic Province (CAMP): A Review. In: Tanner, L. (eds) *The Late Triassic World. Topics in Geobiology*, 46. Springer, https://doi.org/10.1007/978-3-319-68009-5_4
- Dupuy, C., Dostal, J. (1984). Trace element geochemistry of some continental tholeiites. *Earth and Planetary Science Letters*, 67, 61-69. [https://doi.org/10.1016/0012-821X\(84\)90038-4](https://doi.org/10.1016/0012-821X(84)90038-4)
- Fagny Mefie, AFM., Jacques-Marie, B., Faarouk, NO., d'Aquin, LGT., Samira, NM., (2019). Petrology and Geochemistry of Hama Koussou Dolerite Dyke Swarms (North Cameroon, Central Africa). *Journal of Geography, Environment and Earth Science International*, 23(3), 1-19. <https://doi.org/10.9734/jgeesi/2019/v23i330170>.
- Fitton, J. G., Saunders, A. D., Larsen, L. M., Hardarson, B. S., Norry, M. J. (1998). Volcanic rocks from the southeast Greenland margin at 63 N: composition, petrogenesis and mantle sources. In: Saunders, A.D., Larsen, H.C., Wise, S.W., Jr. (Eds.), *Ocean Drilling Program Scientific Results*, vol. 152, pp. 331-350.
- Floyd, P. A., Winchester, J. A. (1975). Magma type and tectonic setting discrimination using immobile elements. *Earth and Planetary Science Letters*, 27(2) : 211-218. [https://doi.org/10.1016/0012-821X\(75\)90031-X](https://doi.org/10.1016/0012-821X(75)90031-X)

- Genik, G. J. (1992). Regional framework, structural and petroleum aspects of rift basins in Niger, Chad and the Central African Republic (C.A.R.). *Tectonophysics*, 213, 169-185.
[http://dx.doi.org/10.1016/0040-1951\(92\)90257-7](http://dx.doi.org/10.1016/0040-1951(92)90257-7)
- Guiraud, R., Maurin, J. C. (1992). Early cretaceous rifts of western and Central Africa: An overview. In: P.A. Ziegler: (Editor). *Geodynamics of Rifting, Volume II. Case 1 history studies on Rifts: North and South America, Africa-Arabia*. *Tectonophysics*, 21, 3:153-368.
[http://dx.doi.org/10.1016/0040-1951\(92\)90256-6](http://dx.doi.org/10.1016/0040-1951(92)90256-6)
- Hellman, P. I., Smith, R. E., Henderson, P. (1979). The mobility of rare earth elements: Evidence and implications from selected terrains affected by burial metamorphism. *Contributions to Mineralogy and Petrology*, 71, 23-44. <https://doi.org/10.1007/BF00371879>
- Hofmann, A. W., Jochum, K. P., Seufert, M., White, W. M. (1986). Nb and Pb in oceanic basalts: new constraints on mantle evolution. *Earth and Planetary Science Letters*, 79, 33-45.
[https://doi.org/10.1016/0012-821X\(86\)90038-5](https://doi.org/10.1016/0012-821X(86)90038-5)
- Hughes, C. J. (1973). Spilites, keratophyres and the igneous spectrum. *Geological Magazine*, 109, 513-527. <https://doi.org/10.1017/S0016756800042795>
- Hynes, A. (1980). Carbonatization and mobility of Ti, Y and Zr in Ascot Formation metabasalts, southeast Quebec. *Contributions to Mineralogy and Petrology*, 75, 79-87.
<https://doi.org/10.1007/BF00371891>
- Isseini, M., André-Mayer, A. S., Vanderhaeghe, O., Barbey, P., Deloule, E. (2012). A-type granites from the Pan-African orogenic belt in south-western Chad constrained using geochemistry, Sr-Nd isotopes and U-Pb geochronology. *Lithos*, 153, 39-52.
<https://doi.org/10.1016/j.lithos.2012.07.014>
- Le Maitre, R. W., (Ed.) (2002). *Igneous Rocks, a Classification and Glossary of Terms*. (Recommendations of the International Union of Geological Sciences Sub commission on the Systematics of Igneous Rocks. Cambridge University Press, P.252.
<http://dx.doi.org/10.1017/CBO9780511535581>
- Marcelot, G., Dupuy, C., Dostal, J., Rancon, JP, Puelet A (1989). Geochemistry of mafic volcanic rocks from the Lake Kivu (Zaire and Rwanda) section of the western branch of the African Rift. *Journal of Volcanology and Geothermal Research*, 39(1), 73-88. [http://dx.doi.org/10.1016/0377-0273\(89\)90022-X](http://dx.doi.org/10.1016/0377-0273(89)90022-X)
- Maurin, J. C., Guiraud, R. (1990). Relationships between tectonics and sedimentation in the Barremo-Aptian intra- continental basins of Northern Cameroon. In: CA Kogbe and J. Lang (Editors), *African Continental Phanerozoic Sediments*. *Journal of African Earth Sciences*, 10 (1/2):331-340.
[https://doi.org/10.1016/0899-5362\(90\)90064-L](https://doi.org/10.1016/0899-5362(90)90064-L)
- McDonough, W. F., Sun, S. S. (1995). The composition of the Earth. *Chemical Geology*, 120, 223-253.
[https://doi.org/10.1016/0009-2541\(94\)00140-4](https://doi.org/10.1016/0009-2541(94)00140-4)
- Miyashiro, A., (1978). Nature of alkalic volcanic rock series. *Contributions to Mineralogy and Petrology*, 66, 91-104. <https://doi.org/10.1007/BF00376089>

- Morata, D., Puga, E., Demant, A., Aguirren, L. (1997). Geochemistry and tectonic setting of the «ophites» from the external zones of the Betic Cordilleras (S. Spain). *Estudios Geológicos-madrid*, 53, 107-120. <https://doi.org/10.3989/egeol.97533-4236>
- Muhammad, D., Durrani, R.A., Kassi, A.M., Kakar M.I. (2019). Petrology and geochemistry of dolerite and lamprophyre sills in Mesozoic successions of Khanozai–Muslim Bagh area, northwestern Pakistan. *Arabian Journal of Geosciences*. 2019 Apr;12(8):266. <https://doi.org/10.1007/s12517-019-4446-5>
- Moreau, C., Regnault, J. M., Déruelle, B., Robineau, B. (1987). A new tectonic model for the Cameroon Line, Central Africa. *Tectonophysics*, 141(4), 317-334. [https://doi.org/10.1016/0040-1951\(87\)90206-X](https://doi.org/10.1016/0040-1951(87)90206-X)
- Pearce, J. A.; (2008) Geochemical fingerprinting of oceanic basalts with applications to ophiolite classification and the search for Archean oceanic crust. *Lithos*, 100, 14-48. <https://doi.org/10.1016/j.lithos.2007.06.016>
- Penaye, J., Kroner, A., Toteu, S. F., Van Schmus, W. R., Doumnang, J. C. (2006). Evolution of the Mayo Kebbi region as revealed by zircon dating: an early (ca. 740 Ma) PanAfrican magmatic arc in southwestern Chad. *Journal of African Earth Sciences*, 44, 530-542. <http://dx.doi.org/10.1016/j.jafrearsci.2005.11.018>
- Pfänder, J. A., Münker, C., Stracke, A., Mezger, K. (2007). Nb/Ta and Zr/Hf in ocean island basalts - Implications for crust-mantle differentiation and the fate of Niobium. *Earth and Planetary Science Letters* 254 (1-2), 158-172. <https://doi.org/10.1016/j.epsl.2006.11.027>
- Plank, T. (2005). Constraints from Thorium/Lanthanum on sediment recycling at subduction zones and the evolution of the continents. *Journal of Petrology*, 46, 921-944. <https://doi.org/10.1093/petrology/egi005>
- Poucllet, A., Vidal, M., Doumnang, J. C., Vicat JP, Tchameni, R. (2006). Neoproterozoic crustal evolution in Southern Chad: Pan-African ocean basin closing, arc accretion and late to post-orogenic granitic intrusion. *Journal of African Earth Sciences*, 44, 543-560. <https://doi.org/10.1016/j.jafrearsci.2005.11.019>
- Puffer, J. H. (2003). A reactivated back-arc source for CAMP Magma. In: Hames, W.E., McHone, J.G., Renne, P.R., Ruppel, C. (Eds.), the Central Atlantic Magmatic Province: Insights from Fragments of Pangea, vol. 136. American Geophysical Union Geophysical Monograph, pp. 151-162. <https://doi.org/10.1029/136GM08>
- Saunders, A. D., Storey, M., Kent, R. W., Norry, M. J. (1992). Consequences of plume–lithosphere interactions. In: Storey, B.C., Alabaster, T., Pankhurst, R.J. (Eds.), Magmatism and the Causes of Continental Break-up, vol. 68. Geological Society of London Special Publication, pp. 41-60. <https://doi.org/10.1144/gsl.sp.1992.068.01.04>
- Scott, E. B., Ernst, R. E. (2008). Revised definition of Large Igneous Provinces (LIPs). *Earth-Science Reviews*, 86, 175-202. <https://doi.org/10.1016/j.earscirev.2007.08.008>
- Sengupta, P., Ray, A., Pramanik, S., (2014). Mineralogical and chemical characteristics of newer dolerite dyke around Keonjhar, Orissa: Implication for hydrothermal activity in subduction zone

setting. *Journal of Earth System Science*, 123(4), 887-904. <https://doi.org/10.1007/s12040-014-0440-1>

- Sun SS, McDonough WF (1989) Chemical and isotopic systematics of oceanic basalts: implications for the mantle composition and processes. In: Saunders, A.D., Norry, M.J. (Eds.), *Magmatism in the Ocean Basins*. Geological Society London Publication 42, 313-345. <https://doi.org/10.1144/gsl.sp.1989.042.01.19>
- Taylor, S. R., McLennan, S. M. (1985). *The continental crust: its composition and evolution*. Blackwell, Oxford, UK. 312.
- Toteu, S. F., (1990). Geochemical characterization of the main petrographical and structural units of Northern Cameroon: implications for Pan-African evolution. *Journal of African Earth Sciences*, 10(4), 615-624. [https://doi.org/10.1016/0899-5362\(90\)90028-D](https://doi.org/10.1016/0899-5362(90)90028-D)
- Toteu, S. F., De Wit, M., Penaye, J., Drost, K., Tait, J. A., Houketchang Bouyo, et al. (2022). Geochronology and correlations in the Central African Fold Belt along the northern edge of the Congo Craton: New insights from U-Pb dating of zircons from Cameroon, Central African Republic, and south-western Chad. *Gondwana Research*, 107, 296-324. <https://doi.org/10.1016/j.gr.2022.03.010>
- Toteu, S. F., Penaye, J., Poudjom Djomani, Y. (2004). Geodynamic evolution of the Pan-African Belt in Central Africa with special reference to Cameroon. *Canadian Journal of Earth Sciences*, 41(1), 73 - 85. <http://dx.doi.org/10.1139/e03-079>
- Wang, K., Plank, T., Walker, J. D., Smith, E. I. (2002). A mantle melting profile across the Basin and Range, SW USA. *Journal of Geophysical Research*, 107 (B1), 2017, ECV 5 - 1, 5-21. <https://doi.org/10.1029/2001JB000209>
- Wilson, M., Guiraud, R. (1998). Late Permian to recent magmatic activity on the African Arabian margin of tethys. In: MacGregor, D.S., Moody, R.T.J., Clark-Lowes, D.D. (Eds.), *Petroleum Geology of North Africa*, vol. 132. *Geological Society*, London, Special Publication, pp. 231-263. <https://doi.org/10.1144/GSL.SP.1998.132.01.14>